

## Tunable midinfrared source by difference frequency generation in bulk periodically poled $\text{KTiOPO}_4$

K. Fradkin,<sup>a)</sup> A. Arie, A. Skliar, and G. Rosenman

*Department of Electrical Engineering—Physical Electronics, Faculty of Engineering, Tel Aviv University, 69978 Tel Aviv, Israel*

(Received 27 October 1998; accepted for publication 14 December 1998)

We demonstrate quasi-phase-matched difference frequency generation in periodically poled  $\text{KTiOPO}_4$ . A midinfrared (3.2–3.4  $\mu\text{m}$ ) idler with a power level of 0.17  $\mu\text{W}$  is generated by mixing a Nd:YAG laser and tunable external cavity laser near 1550 nm which is amplified by an erbium-doped fiber amplifier. The wavelength, temperature, and angle tuning characteristics of this device are determined. The experimental results are used to derive a Sellmeier equation with improved accuracy in the midinfrared range for the extraordinary refractive index of flux-grown  $\text{KTiOPO}_4$ . © 1999 American Institute of Physics. [S0003-6951(99)04007-3]

There is considerable interest in developing sources in the midinfrared range for selective and sensitive measurements of trace-gas concentrations. Since the fundamental vibrational modes of most of the molecules lie in the 2–20  $\mu\text{m}$  wavelength region, infrared spectroscopy using tunable narrow-band sources provides a convenient and real-time method of detection for most gases. Difference frequency mixing in nonlinear materials is a powerful way of producing midinfrared coherent sources using compact and efficient lasers which presently exist mainly in the visible and near-infrared region. Other possible infrared sources for similar applications were reviewed in Refs. 1–3.

Diode-based continuous-wave difference frequency generated (DFG) spectroscopic sources were already demonstrated in the 3–5  $\mu\text{m}$  region with  $\text{AgGaSe}_2$ ,<sup>1</sup>  $\text{LiNbO}_3$ ,<sup>4</sup> and  $\text{AgGaS}_2$ .<sup>5</sup> Electric field poling of ferroelectric crystals opened new possibilities for quasi-phase-matched (QPM) difference frequency generation. These processes can be noncritically phase matched, are highly efficient, and phase matching of the idler wavelength can be achieved using an appropriate QPM grating period. Whereas several ferroelectric crystals can be poled by an electric field, up until now mainly periodically poled  $\text{LiNbO}_3$  was used for DFG processes.<sup>2,6</sup> In this letter we report QPM-DFG using a new crystal: periodically poled  $\text{KTiOPO}_4$  (PP-KTP),<sup>7,8</sup> which was already used before for second-harmonic generation<sup>8</sup> and  $\text{OPO}^9$  processes. After the submission of this paper, difference frequency generation of near-infrared radiation in PP-KTP was also reported.<sup>10</sup> KTP<sup>11</sup> is commercially available from a variety of suppliers at a relatively low price. It exhibits a high damage threshold and is transparent over a large wavelength range: 350–4500 nm.

In addition to providing an alternative method for generating midinfrared radiation, this experiment also enables one to characterize the phase-matching properties of KTP in the midinfrared range, where experimental data are scarce. It is important to emphasize that the published experiments with PP-KTP<sup>7–10</sup> were performed in the visible and near-infrared regions, whereas in this experiment, coherent radia-

tion is generated in the midinfrared range and PP-KTP properties are investigated in this wavelength range. The new data will also be useful for designing other devices in the midinfrared range, e.g., optical parametric oscillators.

The DFG experimental setup employed two compact laser sources: a diode-pumped Nd:YAG laser at 1064 nm (Lightwave Electronics, model 122) and a tunable external cavity diode laser near 1550 nm. The use of a signal source near 1550 nm has great advantages compared to using a visible or near-infrared diode. It enables one to use a wide range of photonics devices developed for this wavelength range, including optical fibers, erbium-doped fiber optic amplifiers, and fiber-coupled diagnostics equipment. Two diode lasers were used: 1490–1568 nm (New-Focus, model 6200) or a fiber-coupled laser, 1400–1600 nm (Hewlett-Packard, model 8168C) with an external fiber-polarization controller. The beams of the pump and signal lasers were combined collinearly using a polarizing beamsplitter and focused into an uncoated 0.5-mm-thick, flux-grown KTP crystal, periodically poled over 10 mm out of its total length of 14 mm. The crystal had three different periodic domain gratings fabricated by low-temperature electric field poling<sup>7</sup> with the following periods: 35.7, 36.3, and 36.8  $\mu\text{m}$ .

Our configuration used the largest nonlinear coefficient in KTP,  $d_{33} = 14.9 \text{ pm/V}$ .<sup>8</sup> Quasi-phase-matched idler wave radiation near  $\sim 3.3 \mu\text{m}$  was generated in the PP-KTP crystal and was refocused with a single uncoated  $\text{CaF}_2$  lens (focal length 100 mm) onto a 1-mm-diam liquid-nitrogen-cooled HgCdTe detector (Fermionics, model PV-6-1) with a cold spectral filter, designed to fit the generated wavelengths. Cooling of this filter is required in order to reduce its thermal emission. The detector, which was used in the photovoltaic mode, exhibited a noise-equivalent power of  $\sim 1 \text{ pW}/\sqrt{\text{Hz}}$ . A tilted uncoated germanium flat was placed immediately in front of the detector to block the pump and signal beams. The signal beam was chopped at a rate of 1.5 kHz, and the idler signal was detected with a lock-in-amplifier. The operating wavelengths of the pump and signal lasers were measured using a Burleigh WA-20 wavemeter with a spectral accuracy of  $\sim 1 \text{ pm}$ .

With 222 mW Nd:YAG power at 1064.4 nm and 3.4

<sup>a)</sup>Electronic mail: kerenfr@post.tan.ac.il

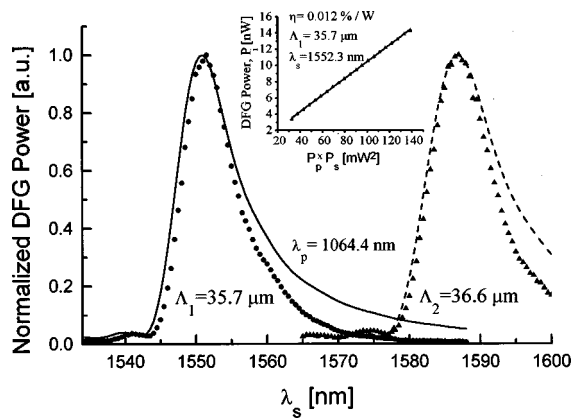


FIG. 1. Measurement of normalized DFG power as a function of the signal wavelength, near room temperature, for two grating periods: 35.7  $\mu\text{m}$  (circles) and 36.6  $\mu\text{m}$  (triangles). The solid and dashed lines are calculated according to the new Sellmeier coefficients, see Eq. (1). Inset: Measurement of DFG conversion efficiency in a 10-mm-long PP-KTP crystal.

mW of diode power at 1552.3 nm incident on the uncoated mixing crystal with period 35.7  $\mu\text{m}$ , a maximum idler power of 24 nW was measured at the detector. Taking into account the transmission of the cold filter and of the uncoated components in the setup (e.g., the crystal facets, the germanium flat, and the  $\text{CaF}_2$  lens) the measured infrared power indicates a normalized internal conversion efficiency of 0.012%/ (W cm).

Assuming a lossless crystal and focused pump and signal Gaussian beams, the generated idler power is given in Ref. 12. Let us denote  $\mu$  as the ratio of the signal and pump wave vectors ( $\mu = k_s/k_p$ ) and  $\xi$  as the ratio of the crystal length to the confocal parameter. For the lasers used in this experiment  $\mu \approx 0.69$ , and the optimal focusing condition is  $\xi \approx 2.5$ , indicating a desired confocal parameter of 4 mm inside the crystal for each of the two laser sources. This condition was achieved by average beam waists of 19.2  $\mu\text{m}$  for the Nd:YAG laser and 23.3  $\mu\text{m}$  for the tunable diode, both having a slightly elliptic profile.

The calculated internal efficiency according to Ref. 12 is 0.04%/ (W cm) for a lossless crystal, and 0.03%/ (W cm) when the relatively high absorption of KTP in the midinfrared range<sup>13</sup> is taken into account. The remaining discrepancy could be attributed to possible deviations from ideal QPM grating,<sup>14</sup> imperfect spatial overlap of the pump and signal beams inside the nonlinear crystal, a slightly elliptic profile for both of the beams, and possible deviations of pump and signal transverse modes from an ideal Gaussian  $\text{TEM}_{00}$  mode. Nevertheless, the measured normalized efficiency is still comparable with reported efficiencies in other nonlinear materials (e.g., periodically poled  $\text{LiNbO}_3$  in Refs. 2 and 6). Alternatively, assuming the measured efficiency of 0.012%/ (W cm), the effective nonlinear coefficient is  $\approx 5.2 \text{ pm/V}$ .

The DFG power as a function of the signal wavelength at room temperature (25  $^\circ\text{C}$ ) is shown in Fig. 1 for two different grating periods:  $\Lambda_1 = 35.7 \mu\text{m}$  and  $\Lambda_2 = 36.3 \mu\text{m}$ . Negligible power was generated with the 36.8  $\mu\text{m}$  grating period since it required signal wavelengths outside our laser diode range. The full width at half-maximum (FWHM) in means of signal wavelength for the 35.7 and 36.3  $\mu\text{m}$  gratings are 8.4 and 10.3 nm, accordingly (which are equivalent

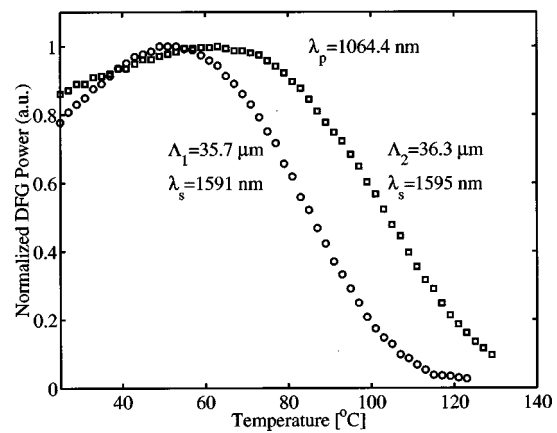


FIG. 2. Measurement of normalized DFG power as a function of the PP-KTP crystal temperature for two grating periods: 35.7  $\mu\text{m}$  (circles) and 36.6  $\mu\text{m}$  (squares).

to a FWHM of 40 and 42.7 nm in means of idler wavelength). The asymmetry of the curve is a result of the tightly focused Gaussian beams.<sup>10,15</sup>

The DFG power as a function of the crystal temperature is shown in Fig. 2 for both of the grating periods: 35.7 and 36.3  $\mu\text{m}$ . The full temperature width at half-maximum is  $\sim 70 \text{ }^\circ\text{C}$ , which is in poor agreement with the bandwidths calculated according to the published temperature derivative of the refractive index,<sup>16,17</sup>  $\sim 20 \text{ }^\circ\text{C}$ . In addition, the optimum phase-matching idler wavelength could be tuned with temperature. We measured a tuning slope of  $\sim 0.5 \text{ nm}/^\circ\text{C}$ , compared to calculated ones:  $\sim 2.3 \text{ nm}/^\circ\text{C}$ <sup>16</sup> and  $\sim 1.5 \text{ nm}/^\circ\text{C}$ .<sup>17</sup> The relatively large difference between the measured and calculated values of the temperature dependence of the refractive index could be due to the fact that Refs. 16 and 17 include measurements in the visible and near-infrared range only. In order to correctly predict the temperature dependence in the midinfrared range, these measurements should be extended to that region.

In order to gain an order of magnitude in the generated infrared power we used an erbium-doped fiber amplifier (IRE-Polus, model EAD60) at the output of the tunable diode. As a result, the diode power at the input facet of the crystal was increased by a factor of  $\sim 10$ , and the maximum idler power that was generated with the amplifier was increased by a factor of  $\sim 7$  (owing to slight deviations from optimum focusing and polarization) to 0.17  $\mu\text{W}$ .

Several different Sellmeier equations for flux-grown  $\text{KTP}$ <sup>13,18,19</sup> appeared in the literature. For a pump operating wavelength of 1064.4 nm at room temperature, the Sellmeier equation of Kato<sup>13</sup> gives the closest estimation to the measured data: 1487  $\mu\text{m}$  for a period of 35.7  $\mu\text{m}$  and 1516 nm for a period of 36.3  $\mu\text{m}$ . However, it is still insufficient in predicting the experimentally measured signal wavelengths 1552.3 nm and 1586.9 nm, accordingly.

We have also measured the angle-dependent phase-matching wavelength of our crystal, by placing the crystal on a rotation stage. This enabled us to achieve phase matching for effectively longer periods, depending on the angle between the incident beams and the perpendicular to the crystal's input facet. Angles in the range  $-10^\circ$  to  $10^\circ$  were measured. This range was limited by the width (2 mm) of the

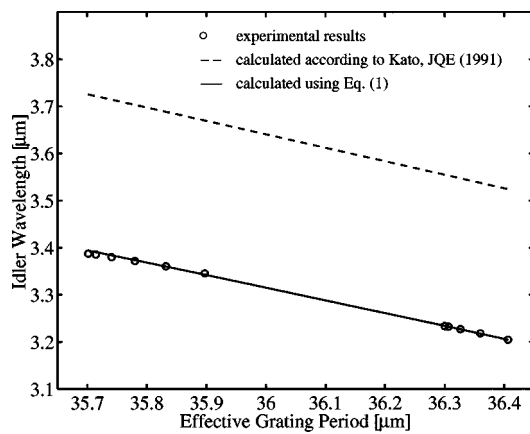


FIG. 3. The generated idler wavelength as a function of the effective grating period.

periodically poled region for each grating, and can be easily extended using a wider region.

Figure 3 shows the idler wavelength at phase matching for each of the effective grating periods. We used the new experimental results to recalculate the Sellmeier coefficients. Using our measured points in the midinfrared wavelengths and previously measured data from Ref. 18 for the refractive index in the visible and near-infrared range we initially attempted to represent the refractive index data in a form similar to the one previously used in Ref. 18, which includes a single pole in the deep ultraviolet. We adjusted the parameters by least-squares data fitting, using the Gauss–Newton method. Since most of the previous measurements of the index of refraction of KTP were performed at wavelengths in the visible and near-infrared range only, we could not predict accurately enough the index of refraction for the signal and for the idler. We therefore iteratively searched for pairs ( $n_s, n_i$ ) that would satisfy both the phase-matching condition and obey the general form of the Sellmeier equation for each grating period. The resulting equation predicted the phase-matching data with reasonable accuracy, but still included systematic residuals. We thus added a second pole in the midinfrared region to the Sellmeier equation in the form of

$$n_z^2 = A + \frac{B}{1 - C/\lambda^2} + \frac{D}{1 - E/\lambda^2} - F\lambda^2 \quad (1)$$

and repeated the fitting procedure. We found that the sum of the square of the residuals was reduced by a factor of 10 with the additional pole. The parameters of the fit are as follows:  $A = 2.12725$ ;  $B = 1.18431$ ;  $C = 5.14852 \times 10^{-2}$ ;  $D = 0.6603$ ;  $E = 100.00507$ ;  $F = 9.68956 \times 10^{-3}$ ; where  $\lambda$  is given in microns. No significant improvement in the fit was obtained when we added a third pole either in the far-infrared or in the deep-ultraviolet range. With Eq. (1), all of the generated idler wavelengths were predicted with a deviation smaller than 0.2%.

We used the new Sellmeier coefficients to calculate theoretically the expected phase-matching curves at room temperature (25 °C). These curves appear in Fig. 1 together

with the measured data. Without any further adjustment we could accurately predict the location of the maximum DFG signal and the first shorter wavelength sideband.

In conclusion, we have demonstrated a PP-KTP-based widely tunable cw single-frequency DFG source operating at midinfrared region. This compact and robust source is suitable for high-resolution spectroscopy in the midinfrared, where many of the interesting spectroscopy molecules exhibit their strongest absorption lines. By using the appropriate QPM gratings, the whole tuning range of the tunable laser can be used to generate a continuous source over an extremely wide range ( $\sim 3.2$ – $4.4 \mu\text{m}$ ). By replacing the liquid-nitrogen-cooled detector with a thermoelectric-cooled detector, the need for liquid nitrogen can be eliminated, and the device described here can serve as a room-temperature spectrometer in the midinfrared range. Typical values for the noise-equivalent power of thermoelectric-cooled detectors are higher by an order of magnitude compared to those of nitrogen-cooled detectors, resulting in a signal-to-noise ratio of  $\sim 10^4$  (instead of  $\sim 10^5$ ), which is still sufficient for most applications. The output power as a function of the input beams power was investigated, giving a conversion efficiency of  $\sim 0.012\%$  W/cm, which is comparable with results obtained with other crystals in this wavelength range. The efficiency can be further improved using other isomorphs of KTP with higher transmission in the infrared range, e.g.,  $\text{KTiOAsO}_4$  and  $\text{RbTiOAsO}_4$ .

- <sup>1</sup>U. Simon, Z. Benko, M. W. Sigrist, R. F. Curl, and F. K. Tittel, *Appl. Opt.* **32**, 6650 (1993).
- <sup>2</sup>T. Topfer, K. P. Petrov, Y. Mine, D. Jundt, R. F. Curl, and F. K. Tittel, *Appl. Opt.* **36**, 8042 (1997).
- <sup>3</sup>C. Sirtori, J. Faist, F. Capasso, D. L. Sivco, A. L. Hutchinson, and A. Y. Cho, *IEEE Photonics Technol. Lett.* **9**, 294 (1997).
- <sup>4</sup>M. Seiter, D. Keller, and M. W. Sigrist, *Appl. Phys. B: Lasers Opt.* **67**, 351 (1998).
- <sup>5</sup>K. P. Petrov, S. Waltman, U. Simon, R. F. Curl, F. K. Tittel, E. J. Dlugokensky, and L. Hollberg, *J. Appl. Phys. B* **61**, 553 (1995).
- <sup>6</sup>L. Goldberg, W. K. Burns, and R. W. McElhanon, *Appl. Phys. Lett.* **67**, 2910 (1995).
- <sup>7</sup>G. Rosenman, A. Skliar, D. Eger, M. Oron, and M. Katz, *Appl. Phys. Lett.* **73**, 3650 (1998).
- <sup>8</sup>A. Arie, G. Rosenman, V. Mahal, A. Skliar, M. Oron, M. Katz, and D. Eger, *Opt. Commun.* **142**, 265 (1997).
- <sup>9</sup>A. Garashi, A. Arie, A. Skliar, and G. Rosenman, *Opt. Lett.* **23**, 1739 (1998).
- <sup>10</sup>G. M. Gibson, G. A. Turnbull, M. Ebrahimzadeh, M. H. Dunn, H. Karlsson, G. Arvidsson, and F. Laurell, *Appl. Phys. B: Lasers Opt.* **67**, 675 (1998).
- <sup>11</sup>D. Bierlein and H. Vanherzeele, *J. Opt. Soc. Am. B* **6**, 622 (1989).
- <sup>12</sup>T. B. Chu and M. Broyer, *J. Phys.* **46**, 523 (1985).
- <sup>13</sup>K. Kato, *J. Quantum Electron.* **27**, 1137 (1991).
- <sup>14</sup>M. M. Fejer, G. A. Magel, D. H. Jundt, and R. L. Byer, *IEEE J. Quantum Electron.* **28**, 2631 (1992).
- <sup>15</sup>S. Guha, F.-J. Wu, and J. Falk, *IEEE J. Quantum Electron.* **QE-18**, 907 (1982).
- <sup>16</sup>W. Wiechmann, S. Kubota, T. Fukui, and H. Masuda, *Opt. Lett.* **18**, 1208 (1993).
- <sup>17</sup>K. Kato, *J. Quantum Electron.* **28**, 1974 (1992).
- <sup>18</sup>T. Y. Fan, C. E. Huang, B. Q. Hu, R. C. Eckardt, Y. X. Fan, R. L. Byer, and R. S. Feigelson, *Appl. Opt.* **26**, 2390 (1987).
- <sup>19</sup>D. W. Anthon and C. D. Crowder, *Appl. Opt.* **27**, 2650 (1988).